Published in final edited form as:
Biochemistry. 2009 February 10; 48(5): 1047–1055. doi:10.1021/bi8020718.

Monovalent cation binding in the minor groove of DNA A-tracts†

Qian Dong‡, **Earle Stellwagen**, and **Nancy C. Stellwagen***
Department of Biochemistry, University of Iowa, Iowa City, IA

Abstract

The binding of five different monovalent cations to DNA oligomers containing A-tracts, runs of four or more contiguous adenine residues, has been measured by capillary electrophoresis, using the Replacement Ion method. In this method, a non-binding cation in the background electrolyte is gradually replaced by a binding cation, keeping the ionic strength of the solution constant. Monovalent cation binding reduces the effective charge of an A-tract-containing soligomer, decreasing its free solution mobility. The cations bind in the A-tract minor groove, because the binding site can be blocked by the minor groove binding drug netropsin. Li^+, NH_4^+ and $Tris^+$ ions bind to A-tracts with similar affinities; the binding of Na^+ ions is weaker, and K^+ ion binding is highly variable. Each A-tract appears to bind one monovalent cation upon saturation of the binding site(s). For a given cation, the apparent dissociation constants depend on A-tract sequence and orientation, but not on the phasing of the A-tracts with respect to the helix repeat. Differences in the cooperativity of binding of the various cations to A-tracts with different sequences suggest that monovalent cation binding may be coupled with a conformational transition leading to the formation of the characteristic narrow minor groove A-tract structure.

Keywords

monovalent cations; binding; DNA; A-tracts; capillary electrophoresis

X-ray diffraction and NMR studies, as well as molecular dynamics simulations, have shown that monovalent cations bind in the minor groove of DNA A-tracts, runs of four or more contiguous adenine or thymine residues (reviews: [1–7]). The grooves are only partially occupied by cations; the remainder of each groove is filled with water molecules ([8–11]). In the Dickerson-Drew dodecamer (12), which has an AATT sequence motif flanked by GC residues, monovalent cations are located at the ApT step in the minor groove ([8–10, 13–16]) and near the guanine residues in the major groove ([3, 10, 17]), two sites with relatively deep electronegative potentials (18). Since the bound cations can exchange readily with each other, with other cations in the bulk solution and with water molecules in the grooves, the cations appear to remain hydrated in the bound state ([5, 7, 19, 20]).

Capillary electrophoresis (CE) is another technique that can be used to measure monovalent cation binding to DNA A-tracts ([21, 22]). The free solution mobility of an analyte, μ, is determined by the ratio between its effective charge, *Q*, and its frictional coefficient, *f*, as shown in eq 1:

†This work was supported in part by grant GM061009 from the National Institute of General Medical Sciences and grant CHE0748271 from the Analytical and Surface chemistry Program of the National Science Foundation (to N.C.S.).

*Corresponding author. Tel: (319-335-7896.fax: (319-335-9570. E-mail: nancy-stellwagen@uiowa.edu.
‡Present address: Department of Internal Medicine, University of Iowa, Iowa City, IA 52242.

$$\mu = Q/f = Q\,D_t/k_B T \quad (1)$$

Here, D_t is the translational diffusion coefficient of the analyte, k_B is Boltzmann's constant and T is the absolute temperature. Since the diffusion coefficients of small DNA oligomers containing the same number of base pairs are independent of sequence *(23)*, differences in the free solution mobilities of different oligomers are a direct measure of cation binding.

In our first study *(21)*, we showed that 20-bp oligomers containing phased A- or T-tracts migrated more slowly in Tris buffer solutions than a 20-bp oligomer without A-tracts, suggesting that the preferential binding of $Tris^+$ ions decreased the effective net charge of the A-tract-containing oligomers. In a second study (22), we showed that the free solution mobility of a stably curved, 199-bp restriction fragment from the VP1 gene of simian virus 40 (SV40) decreased progressively with the increasing number of A-tracts in a "curvature module" in the center of the fragment, again indicating that A-tracts bind $Tris^+$ ions. More recently (24), we have combined the CE measurements with estimates of the translational diffusion coefficients of the SV40 curvature module mutants to show that each A-tract in the curvature module is occupied about 30% of the time by $Tris^+$ ions.

The previous studies were not designed to measure the affinity of cation binding to DNA A-tracts. Here we address this question, using a variation of affinity capillary electrophoresis called the Replacement Ion (RI) method (25) to quantitate the binding of different cations to A-tracts with different sequences. In the RI method, a large, presumably non-binding cation, such as the tetrapropylammonium (TPA^+) ion, is gradually replaced by a binding cation, such as Li^+, Na^+, K^+, NH_4^+, or $Tris^+$, keeping the total ionic strength of the solution constant. The constant ionic strength prevents the large variation of the mobility with ionic strength (26, 27) from obscuring the small mobility differences due to cation binding. The RI method has previously been used to study the non-specific binding of monovalent cations to a random-sequence, 26-bp DNA oligomer (25). The random-sequence oligomer, and presumably all DNA oligomers, bind monovalent cations in a saturable manner, with apparent dissociation constants ranging from 71 mM for $Tris^+$ to 173 mM for Na^+ and K^+. These bound cations appear to correspond to the strongly correlated, "tightly bound" ions recently postulated to be trapped on the DNA surface by the strong electrostatic field of the phosphate residues (28).

The sequence-specific binding of monovalent cations to DNA A-tracts would occur in addition to any non-specific cation binding. Therefore, the difference in mobility between an A-tract-containing oligomer and a random-sequence oligomer containing the same number of base pairs can be attributed unambiguously to cation binding to the A-tract(s). Such mobility differences can be determined very accurately, because they are measured in the same solution at the same time under exactly the same ionic conditions. The mobility differences measured as a function of binding ion concentration are then used to calculate the apparent dissociation constants, as described previously (25).

The results indicate that Li^+, NH_4^+ and $Tris^+$ ions bind to DNA A-tracts with similar affinities, Na^+ ions bind more weakly, and the binding of K^+ ions is variable. The binding affinities depend on A-tract sequence, sequence context and orientation, but do not depend on the phasing of the A-tracts with respect to the helix repeat. Each A-tract appears to bind one monovalent cation upon saturation of the binding site(s). The sigmoidal binding curves observed in most of the mobility profiles suggest that monovalent cation binding in the A-tract minor groove may be coupled with a conformational transition leading to the characteristic narrow minor groove structure.

MATERIALS AND METHODS

DNA samples

All DNA oligomers used in these studies contained 26 base pairs (bp), with GC bp at the ends to minimize fraying. The oligomers contained one or two A-tracts of various lengths; the total A+T content was either 46% or 62%. The oligomers are identified in the following text by acronyms denoting the A-tract sequence and phasing (if more than one A-tract was present), followed by a hyphen and a number indicating the % A+T in the oligomer. The sequences of the oligomers and their acronyms are given in the first two columns of Table 1 and Table 2. For clarity, the A-tracts in each oligomer are underlined.

All oligomers were synthesized by IDT (Integrated DNA Technologies, Coralville, IA) and purified by polyacrylamide gel electrophoresis. Duplexes were prepared by mixing equimolar quantities of the complementary strands (1 μg/μL) in 10 mM Tris chloride buffer, pH 8.0, heating to 94°C for 5 minutes and slowly cooling to room temperature. For sequences which had a significant tendency to form hairpins, it was necessary to extend the cooling period for several hours or overnight. All duplexes described here exhibited single bands in 9.3%T, 3% C polyacrylamide gels, prepared as described previously (29), and sharp, nearly Gaussian-shaped peaks in the CE electropherograms. Hence, no truncated failure sequences or unreacted single-strands were present. Concentrated stock solutions of the duplexes in 10 mM Tris-Cl buffer were stored in a freezer at −20°C; the samples were diluted with water to concentrations of 10–50 ng/μL for the CE experiments. The mobilities were independent of concentration within this range.

Netropsin-DNA complexes were prepared by adding netropsin (4 μM) to samples containing a mixture of RA-46 and A4T1in-62 (2 μM each), and allowing the solutions to stand for one hour at room temperature to reach equilibrium. The A-tract/netropsin molar ratio was 1:1, because oligomer A4T1in-62 contains two A-tracts.

Buffers

All buffers contained 200 mM diethylmalonic acid (DM) as the background electrolyte, titrated to pH 7.3, the pKa of the second carboxyl group, with a concentrated solution of Tris base or the hydroxide of Li^+, Na^+, K^+, NH_4^+, or TPA^+. Because the second carboxyl group in DM is half ionized at pH 7.3, the total cation concentration in each solution was 300 mM; the ionic strength was 400 mM. Solutions with mixed cations were prepared by combining appropriate volumes of the individual buffer solutions. The actual cation concentration in each solution was calculated from the measured pH (Radiometer pHM82 Standard Meter, Copenhagen) and the pKa of DM, using the Henderson-Hasselbalch equation. Diethylmalonic acid $[(CH_3CH_2)_2C(COOH)_2]$ and the hydroxides of the various cations were purchased from Sigma-Aldrich (St. Louis, MO). Tris base was purchased from Research Products International Corp. (Mt. Prospect, IL).

Capillary Electrophoresis

Capillary zone electrophoresis measurements were carried out with a Beckman Coulter P/ACE System MDQ Capillary Electrophoresis System (Fullerton, CA), run in the reverse polarity mode (anode on the detector side) with UV detection at 254 nm, as described previously (30). Migration times and peak profiles were analyzed using the 32 Karat™ software. The capillaries were LPA (Linear Poly-Acrylamide) internally coated capillaries from Bio-Rad (Hercules, CA). Coated capillaries are used to minimize the electroosmotic flow (EOF) of the solvent; previous studies have shown that polyacrylamide coatings do not affect the observed mobilities (31). The capillaries were 40.0 cm in total length, with external diameters of 375

μm and internal diameters of 75 μm. The distance from the inlet to the detector, L_d, was 29.8 cm. The capillaries were mounted in a liquid-cooled cartridge thermostated at 20° ± 0.1°C.

The capillary was conditioned at the beginning of each day by rinsing with running buffer (called the background electrolyte, BGE) for 5 min at high pressure (25 p.s.i., 0.17 Mpa). Between runs, the capillary was rinsed with the BGE at 25 p.s.i. for 2 min. The capillary was rinsed with deionized water at 25 p.s.i. for 5–10 min at the end of each day and filled with deionized water overnight. The DNA samples were hydrodynamically injected into the capillary by applying low pressure (0.5 p.s.i., 0.0035 MPa) for 3 s. The injection volume was 22 nL, giving a sample plug 0.51 cm in length (1.7% of total capillary length). Particular care was taken to equalize the liquid levels in the buffer reservoirs to prevent hydrodynamic flow between the two buffer chambers. The buffers in all vials were replaced after 4–6 runs. The electric field was typically 90–110 V/cm (3.5 to 4.5 kV applied voltage); the mobilities and mobility differences were independent of the applied field within this range. The current typically ranged between 40 and 70 μA for various experiments. Control experiments showed that heating within the capillary was negligible under these conditions.

The residual EOF in the capillary was measured every day by a fast pressure-assisted method (32), using 40 mM acrylamide as the analyte. The EOF of a new capillary was typically ~5×10^{-6} cm^2/Vs. When the EOF increased to ~1×10^{-5} cm^2/Vs, indicating deterioration of the capillary coating, the capillary was replaced. Since the EOF was negligibly small, DNA electrophoretic mobilities, μ, were calculated from eq 2:

$$\mu = L_d / E\,t \tag{2}$$

where L_d is the distance to the detector (in cm), E is the electric field strength (in V/cm) and t is time required for the sample to migrate from the inlet to the detector (in seconds). The average standard deviation of the mobilities measured for a given DNA sample on the same or different days was typically ±0.2%.

In the present case, the quantity of greatest interest was not the apparent absolute mobility, μ, but the difference in mobility between an A-tract-containing oligomer and a random-sequence oligomer of the same size, as shown by eq 3:

$$\Delta\mu = \mu(\text{A-tract oligomer}) - \mu(\text{random oligomer}) \tag{3}$$

Defined in this manner, the Δμ values are negative when cations are bound because the mobility of A-tract-containing oligomer is smaller than the mobility of the random-sequence control. For brevity, all mobilities and mobility differences are expressed in mobility units, m.u.; 1 m.u. = 1×10^{-4} cm^2 /Vs.

Measurement of cation binding using the Replacement Ion (RI) method

In the Replacement Ion (RI) method (25), the ionic strength of the solution is kept constant by gradually replacing a non-binding ion in the BGE by a binding ion, and comparing the mobility of binding and non-binding oligomers as a function of binding ion concentration. In this work TPA^+ was used as the non-binding ion, Li^+, Na^+, K^+, NH_4^+, and $Tris^+$ were used as the binding ions, and oligomer RA-46 was used as the non-binding oligomer. If cation binding does not occur, no mobility differences are observed between the test oligomer and oligomer RA-46. When binding occurs, the mobility differences gradually increase (in absolute value) with increasing cation concentration; the mobility differences observed as a function of binding ion concentration are called mobility profiles, for brevity. The dissociation constants (K_D) were

determined either from the midpoints of the transitions in the mobility profiles or by non-linear curve fitting, using SigmaPlot. A three parameter Hill equation, shown in eq 4, was usually used to fit the data.

$$\Delta\mu = \frac{\Delta\mu_{max}[M^+]^n}{K_D{}^n + [M]^n} \quad (4)$$

Here, Δμ is the mobility difference observed at a ligand concentration of $[M^+]$, $\Delta\mu_{max}$ is the mobility difference that would be observed upon saturation of the binding site(s), K_D is the dissociation constant, and *n* is the cooperativity parameter (33). Since the dissociation constants are population averages that could reflect cation binding to different positions within an A-tract or to different A-tracts in the same oligomer, the results are described as apparent dissociation constants, $^{app}K_D$, in the following text. The $^{app}K_D$ values calculated from the mobility profiles or the transition midpoints agreed with each other and were usually reproducible within ±10% in replicate experiments; the mobility differences observed upon saturation of the binding site(s), $\Delta\mu_{max}$, were also usually reproducible within ±10%.

RESULTS AND DISCUSSION

Characterization of oligomers by capillary electrophoresis

Samples containing the random-sequence oligomer RA-46 and an A-tract-containing oligomer were electrophoresed in BGEs containing TPA^+ as the non-binding ion, a cation such as Li^+ as the binding ion, or mixtures of the two ions. The mobility profiles were usually measured from pure TPA^+ to pure Li^+; identical results were obtained if the titration was carried out in the opposite direction. Typical electropherograms observed for the titration of oligomer A_4T_4'in-62 with Li^+ are illustrated in Figure 1A. Oligomers RA-46 and A_4T_4'in-62 migrated as a single peak in pure TPA^+ (left-most panel). The peak gradually resolved into two peaks with increasing $[Li^+]$, as shown in the panels to the right. For clarity, the $[Li^+]$ is indicated beneath each panel. Separate control experiments, carried out either by "spiking" (increasing the concentration of one of the oligomers and repeating the measurement) or by measuring the oligomers separately in solutions containing only Li^+ ions, showed that the more slowly migrating peak observed at high $[Li^+]$ was A_4T_4'in-62. Hence, Li^+ ions bind preferentially to A_4T_4'in-62, reducing its effective charge and thereby reducing its mobility. Similar mobility patterns, differing only in quantitative detail, were observed for most of the other A-tract-containing oligomers.

Completely different results were observed when the sample contained two random-sequence oligomers, as shown in Figure 1B. Oligomers RA-46 and R-62 comigrated in pure TPA^+, in BGEs containing various Li^+/TPA^+ ratios and in pure Li^+, indicating that neither oligomer preferentially binds monovalent cations. It is possible that both oligomers bind Li^+ ions in a non-sequence-specific manner, as observed previously (25). However, any non-sequence-specific binding must be the same for both oligomers, because they comigrate at all $[Li^+]$. Hence, the mobility differences observed between the random-sequence control, RA-46, and an A-tract-containing oligomer can be attributed unambiguously to preferential cation binding by the A-tract(s) in the test oligomer.

Mobility profiles

Migration times corresponding to the maxima observed in the electropherograms of RA-46 and the A-tract-containing oligomers were converted to mobilities using eq 2, and the mobility differences, Δμ, calculated from eq 3. The mobility differences were plotted as a function of the concentration of the binding cation, giving mobility profiles such as those illustrated in

Figure 2. The mobility profiles were very reproducible, as shown for Li^+ ions binding to oligomer A_4T_1in-62 in Figure 2A. Figure 2A also shows that the mobility profiles measured in BGEs containing two different cation concentrations (150 and 300 mM) were superimposable over the common range of $[Li^+]$. Hence, the $^{app}K_D$ values measured here are independent of the particular buffer concentration chosen for the study.

Although the individual mobility profiles were very reproducible, the shapes of the mobility profiles depended on A-tract sequence. For some oligomers, such as A_4T_1in-62 (Figure 2A), the mobility differences increased monotonically (in absolute value) with increasing Li^+ ion concentration, leveling off at a constant plateau value at high $[Li^+]$. This plateau value is defined as $\Delta\mu_{max}$. The titration curves observed for most of the other oligomers, such as A_2T_2-46 and A_5=T_5out-46 (Figure 2B), were qualitatively different. The mobility differences were zero until a threshold concentration of Li^+ was reached, after which the mobility differences increased (in absolute value) until a constant plateau value was reached at high $[Li^+]$. Figure 2B also shows that larger values of $\Delta\mu_{max}$ were observed for oligomers containing two A-tracts rather than one, indicating that greater numbers of Li^+ ions bind to oligomers with two A-tracts.

Identification of the cation binding site

To identify the location of the monovalent cation binding site in the A-tract-containing oligomers, netropsin was added to a solution containing RA-46 and A_4T_1in-62 and titrations were carried out using $Tris^+$ as the binding ion. Netropsin binds to DNA in the A-tract minor groove with an affinity in the low nM range, depending somewhat on A-tract sequence (34–39). Surface plasmon resonance measurements (40) have shown that the on-rate for netropsin binding to an AATT site is $3.0 \times 10^7\ M^{-1}s^{-1}$; the off-rate is $7.5 \times 10^{-2}\ s^{-1}$. Hence, a DNA-netropsin complex is expected to to be stable for the duration of a CE measurement. However, because netropsin contains two positively charged residues, netropsin binding decreases the net charge of an A-tract-containing oligomer. Hence, a mixture of RA-46 and the A_4T_1in-62/netropsin complex exhibits two peaks in TPA^+, a rapidly migrating peak due to RA-46 and a slower peak corresponding to the A_4T_1in-62/netropsin complex (not shown). Within experimental error, the widths of the peaks (full width at half height) were independent of the $TPA^+/Tris^+$ ratio in the BGE.

The mobility profile observed for oligomer A_4T_1in-62 (without netropsin) is illustrated in the upper curve in Figure 3. The mobility difference increased gradually (in absolute value) with increasing $[Tris^+]$ before leveling off at a plateau value of -0.012 ± 0.001 m.u. at high $[Tris^+]$. By contrast, the mobility profile observed for the A_4T_1in-62/netropsin complex was nearly independent of $Tris^+$ concentration, as shown by the lower mobility profile in Figure 3. The average value of $\Delta\mu$ observed for the A_4T_1in-62/netropsin complex at $Tris^+$ concentrations greater than 15 mM was -0.028 ± 0.001 m.u. The constancy of this value is strong evidence for the integrity of the A_4T_1in-62/netropsin complex at high $[Tris^+]$. The conclusion must be drawn that $Tris^+$ ions do not bind preferentially to the A_4T_1in-62/netropsin complex, most likely because the minor groove binding site is blocked by netropsin. Similar results are observed with Li^+ as the binding ion (not shown).

Binding of Li^+ ions to A-tracts with different sequences

Li^+ ions were used to investigate monovalent cation binding to A-tracts with different sequences. Thirteen of the tested oligomers failed to bind monovalent cations; the electropherograms observed for these samples exhibited a single peak at all $[Li^+]$. The acronyms of these oligomers, which denote their A-tract sequences, are: A_3-46, A_3-62, A_4-62, A_5-62, A_4T_2-62, A_3in-62, A_4in-62, A_2T_2in-62, A_1T_4in-62, A_2T_4in-62, A_3T_4in-62, T_2A_2in-62 and T_4A_4in-62. Several conclusions may be drawn from these results. First, A_3-tracts are too short to bind monovalent cations, even when two A_3-tracts occur in phase with the helix repeat.

Other studies have also found that an A_3-tract is too short to exhibit the characteristic A-tract structure (16, 41, 42). Secondly, single A_4- and A_5-tracts do not bind monovalent cations when embedded in an AT-rich oligomer. Thirdly, an A_nT_m sequence motif in a relatively short A-tract must have $n \geq m$, in order to bind monovalent cations. The combined results suggest that monovalent cation binding is a sensitive reporter of whether a given A/T motif has the potential to form the narrow minor groove characteristic of the A-tract structure.

The $^{app}K_D$ values determined for the binding of Li^+ ions to the other tested A-tract-containing oligomers are given in columns 3 of Table 1 and Table 2. Several trends can be noted within the data. First, the $^{app}K_D$ values observed for the various oligomers are independent of A-tract phasing, as shown for oligomer pairs A_5in-46 and A_5out-46 (both $^{app}K_D$ = 71mM), A_5=T_5in-46 and A_5=T_5out-46 (average $^{app}K_D$ = 68 ± 1 mM), A_3T_3in-62 and A_3T_3out-62 (average $^{app}K_D$ = 75 ± 10 mM), and A_4T_4in-62 and A_4T_4out-62 (average $^{app}K_D$ = 59 ± 5 mM). Secondly, the $^{app}K_D$ values are also independent of whether the oligomer contains one or two A-tracts. The $^{app}K_D$ value observed for oligomer A_5-46 (65 mM) is essentially equal to the $^{app}K_D$ values observed for oligomers A_5in-46, A_5out-46, A_5=T_5in-46 and T_5=A_5in-46 (average value, 70 ± 2 mM). In addition, the $^{app}K_D$ value observed for oligomer A_4T_4-62 (68 mM) is close to the average value observed for oligomers A_4T_4in-62, A_4T_4'in-62 and A_4T_4out-62 (average $^{app}K_D$ = 59 ± 4 mM). Thirdly, the $^{app}K_D$ values depend on A-tract orientation. The $^{app}K_D$ values observed for oligomers A_5in-46 and A_4T_4in-62 (67 ± 3 mM) are smaller than the $^{app}K_D$ values observed for oligomers T_5in-46 and A_4T_4/T_4A_4in-62 (both 100 mM). In addition, oligomers A_4T_1in-62 and A_4T_4in-62 bind monovalent cations, while the corresponding oligomers A_1T_4in-62 and T_4A_4in-62 do not.

Finally, oligomers containing A_n-tracts (*e.g.*, A_4-46, A_6-46 and A_4in-46) have smaller $^{app}K_D$ values (46 ± 4 mM) than oligomers containing A_nT_n-tracts of equal length (A_2T_2-46, A_3T_3-46 and A_2T_2in-46, average $^{app}K_D$ = 91 ± 26 mM). This result could be taken to indicate that the ApT step interferes with cation binding. However, oligomer A_4T_1in-62 has the lowest $^{app}K_D$ of all tested oligomers (24 mM), suggesting that a thymine residue following an A-tract actually facilitates cation binding. It is known that the A-tract minor groove progressively narrows in the 5' → 3' direction, reaching a minimum at 4–5 base pairs (43–47). Since monovalent cation binding appears to occur preferentially at the narrowest end of the minor groove (46, 47), the relatively deep electrostatic potential at an ApT step (18) may increase the affinity of monovalent cations for binding to an A_4T_1-tract. Oligomers with longer T-tracts might have larger apparent dissociation constants because a T_n-tract following an ApT step widens the minor groove somewhat (46). In agreement with this hypothesis, the average $^{app}K_D$ observed for oligomers A_4T_2in-62, A_4T_3in-62, A_4T_4in-62, and A_4T_4'in-62 was 63 ± 6 mM, much larger than the $^{app}K_D$ of 24 mM observed for oligomer A_4T_1in-62.

The plateau value of the mobility differences observed at high Li^+ concentrations, $\Delta\mu_{max}$, is a measure of the relative concentration of Li^+ ions bound to the A-tract minor groove upon saturation of the binding site(s). The $\Delta\mu_{max}$ values are given in the last columns of Table 1 and Table 2. Significantly, the $\Delta\mu_{max}$ values observed for oligomers A_4in-46, A_5in-46, A_2T_2in-46, A_3T_3in-46, A_4T_1in-62, A_4T_3in-62, and A_4T_4in-62, each of which contains two A-tracts, were 2.0 ± 0.4 times greater than the $\Delta\mu_{max}$ values observed for the corresponding oligomers with one A-tract: A_4-46, A_5-46, A_2T_2-46, A_3T_3-46, A_4T_1-62, A_4T_4-62 and A_4T_4-62. Hence, each A-tract binds the same number of monovalent cations upon saturation of the binding site(s). In addition, the ratio of the $\Delta\mu_{max}$ values observed for oligomer pairs A_5in-46 and A_5out-46, A_5=T_5in-46 and A_5=T_5out-46, A_3T_3in-62 and A_3T_3out-62, and A_4T_4in-62 and A_4T_4out-62 was 1.0 ± 0.1. Hence, the extent of monovalent cation binding in the A-tract minor groove at saturation is independent of the phasing of the A-tracts with respect to the helix repeat.

Comparison of the binding of different cations to DNA A-tracts

To analyze the dependence of cation binding on the type of monovalent cation, mobility profiles were measured for two representative oligomers, A_4T_1in-62 and A_4T_4'in-62, using Li^+, $Tris^+$, NH_4^+, Na^+ and K^+ as the binding ions. The mobility profiles observed for oligomer A_4T_1in-62 are illustrated in Figures 4A and 4B. The mobility profiles observed in solutions containing Li^+ or NH_4^+ ions were nearly hyperbolic in shape, while the mobility profiles observed for the other three cations were clearly sigmoidal. In addition, the $\Delta\mu_{max}$ value observed with NH_4^+ as the binding ion was ~30% greater than observed for the other cations. For oligomer A_4T_4'in-62, shown in Fig. 5, the mobility profile observed in solutions containing NH_4^+ as the binding ion was nearly hyperbolic in shape; the mobility profiles observed with Li^+, $Tris^+$, and Na^+ as the binding ions were sigmoidal. K^+ ions did not bind to oligomer A_4T_4'in-62 in solutions containing 300 mM cation.

The mobility profiles in Figure 4 and Figure 5 were analyzed using eq 4. The curved lines in Figure 4 and Figure 5 were drawn with these fitting parameters; the ${}^{app}K_D$ and $\Delta\mu_{max}$ values and the cooperativity parameters, *n*, are given in Table 3. NH_4^+, Li^+ and $Tris^+$ ions have similar affinities for binding to oligomer A_4T_1in-62, with an average ${}^{app}K_D$ of 34 ± 9 mM; the binding of K^+ ions is somewhat weaker (${}^{app}K_D$ = 63 mM), and the binding of Na^+ ions is weaker still (${}^{app}K_D$ = 112 mM). For oligomer A_4T_4in-62, NH_4^+ ions have the strongest binding affinity (${}^{app}K_D$ = 35 mM), Li^+ and $Tris^+$ ions bind more weakly (${}^{app}K_D$ = 68 mM), Na^+ ions binds still more weakly (${}^{app}K_D$ = 159 mM), and K^+ ions do not bind in solutions containing 300 mM cation. The results are in reasonable agreement with those of Denisov and Halle (48), who found that monovalent cation binding to an A_2T_2-tract decreased in the order $NH_4^+ \gg K^+ \sim Rb^+ \sim Cs^+ > Na^+$. However, the results also indicate that monovalent cation binding to DNA A-tracts depends on A-tract sequence as well as the identity of the cation.

The average value of $\Delta\mu_{max}$ observed for the binding of Li^+, $Tris^+$, Na^+ and K^+ ions to oligomer A_4T_1in-62 was −0.013 ± 0.001 m.u. The binding of NH_4^+ ions was ~30% higher, suggesting that this cation may have additional binding sites on this oligomer. For oligomer A_4T_4'in-62, the average value of $\Delta\mu_{max}$ was −0.019 ± 0.002 m.u. (when binding was observed). The combined results indicate that the extent of the mobility decrease observed upon saturation of the binding site(s) varies modestly with A-tract sequence and cation identity.

By contrast, the cooperativity of binding depends significantly on A-tract sequence and cation identity, as shown in columns 4 and 7 of Table 3. The binding of NH_4^+ ions to both oligomers, and Li^+ ions to oligomer A_4T_1in-62, was essentially non-cooperative, since the cooperativity parameter *n* was close to 1. However, higher *n* values were observed for the other cations, suggesting that cation binding may be coupled with another effect, such as a conformational transition. It is possible that, with TPA^+ as the only cation in the BGE, many A-tract-containing DNA oligomers exist in an equilibrium between the normal B-form conformation and a conformation with the narrow minor groove characteristic of A-tract-containing oligomers ([12](), [49](), [50]()); this conformation will be called the B' conformation, for brevity. If the B' conformation is the only one capable of binding monovalent cations, cation binding would pull the equilibrium toward this conformation. Molecular dynamics (MD) simulations ([51]()–[53]()) have shown that that the narrow minor groove characteristic of DNA A-tracts cannot exist for any significant length of time without cations to neutralize part of the negative charge on the phosphate residues; cation binding in the minor groove draws the phosphate residues closer together and stabilizes the B' conformation. The results in Table 3 indicate that some cations, especially NH_4^+ and Li^+, are more effective than others in pulling the equilibrium toward (and/or stabilizing) the B' conformation. In addition, some A-tract sequences, such as A_4T_1, bind cations in the minor groove with a higher affinity than other A-tract sequences, suggesting that the equilibrium between the B and B' conformations and/or the effect of monovalent cations on the B ↔ B' conformational equilibrium is sequence specific.

Concentration of bound cations at saturation

The average mobility difference observed at high cation concentrations, $\Delta\mu_{max}$, can be used to estimate the number of cations bound to the A-tract(s) upon saturation of the binding site (s). The oligomers studied here contained 50 charged phosphate residues, since the 5'-ends were not phosphorylated. The electrophoretic mobility observed for the random-sequence oligomer RA-46 in the Tris-DM buffers used here was 1.570 m.u. or, equivalently, 0.0314 m.u. per charged residue. However, counterion condensation theory (54) suggests that the effective charge of DNA is reduced to 24% of the formal charge in solutions containing monovalent cations. Therefore, the mobility observed for oligomer RA-46 corresponds to 0.0075 m.u. per charged residue (0.0314 m.u. × 0.24). The average mobility difference observed for the A_4T_1in-62/netropsin complex at high $Tris^+$ concentrations was −0.028 ± 0.001 m.u. (Figure 3), or −0.014 m.u. per A-tract. The observed mobility reduction is therefore equivalent to a decrease of two charges per A-tract. Since each netropsin contains two positive charges, one netropsin is bound to each A-tract. A similar 1:1 binding stoichiometry has also been observed by others (36–39, 55).

The average value of $\Delta\mu_{max}$ observed for the binding of Li^+, $Tris^+$, NH_4^+, Na^+ and K^+ ions to oligomers A_4T_1in-62 and A_4T_4in-62 (Table 3) was −0.016 ± 0.003 m.u. (when binding was observed), or, equivalently, −0.008 m.u. per A-tract. From the above discussion, this mobility difference corresponds to the binding of 1.1 ± 0.2 cations to each A-tract upon saturation of the binding site(s).

CONCLUDING REMARKS

The results described here have shown that monovalent cations bind to the A-tract minor groove, because the binding site can be blocked by netropsin, a minor groove binding drug. Not all A-tracts bind monovalent cations: A_3-tracts are too short, and isolated A_4- and A_5-tracts, especially when embedded in AT-rich oligomers, often do not bind cations.
The $^{app}K_D$ values observed for oligomers that do bind cations in the minor groove indicate that monovalent cation binding is sequence specific. The $^{app}K_D$ values are independent of the number of A-tracts in the oligomer and the phasing of the A-tracts, but vary with A-tract orientation and the presence or absence of an ApT step in the A-tract. In addition, oligomers containing A_{2n}-tracts exhibit a higher affinity for monovalent cations than oligomers containing A_nT_n-tracts. The $\Delta\mu_{max}$ values, which indicate the extent of cation binding upon saturation of the binding site(s), are two-fold larger when an oligomer contain two A-tracts rather than one; therefore, each A-tract binds the same number of cations at saturation. The affinity of monovalent cation binding depends both on A-tract sequence and cation identity. When binding is observed, the affinity decreases as $NH_4^+ \sim Li^+ \sim Tris^+ > K^+ > Na^+$. Finally, differences in the cooperatively of binding to various A-tracts suggest that monovalent cations can shift the equilibrium between the normal B conformation and the B' conformation toward the latter, leading to the narrow minor groove structure characteristic of DNA A-tracts.

Abbreviations

BGE, background electrolyte; CE, capillary electrophoresis; DM, diethylmalonic acid; EOF, electroosmotic flow; m.u., mobility unit, 1 m.u. = 1×10^{-4} cm^2/Vs; $^{app}K_D$, apparent dissociation constant; RI, Replacement Ion; TPA^+, tetrapropylammonium ion..

REFERENCES

1. Halle B, Denisov VP. Water and monovalent ions in the minor groove of B-DNA oligonucleotides as seen by NMR. Biopolymers 1998;48:210–233. [PubMed: 10699841]

2. McFail-Isom L, Sines CC, Williams LD. DNA structure: cations in charge? Curr. Opin. Struct. Biol 1999;9:298–304. [PubMed: 10361089]
3. McConnell KJ, Beveridge DL. DNA structure: what's in charge? J. Mol. Biol 2000;304:803–820. [PubMed: 11124028]
4. Hud NV, Plavec J. A unified model for the origin of DNA sequence-directed curvature. Biopolymers 2003;69:144–159. [PubMed: 12717729]
5. Marincola FC, Casu M, Saba G, Lai A. ^{23}Na MNR relaxation studies of the Na-DNA/drug interaction. Chemphyschem 2001;2:569–575.
6. Egli M. DNA-cation interactions: quo vadis? Chem. Biol 2002;9:277–286. [PubMed: 11927253]
7. Subriana JA, Soler-López M. Cations as hydrogen bond donors: a view of electrostatic interactions in DNA. Annu. Rev. Biophys. Biomol. Struct 2003;32:27–45. [PubMed: 12598364]
8. Tereshko V, Minasov G, Egli M. A 'hydrat-ion' spine in a B-DNA minor groove. J. Am. Chem. Soc 1999;121:3590–3595.
9. Woods KK, McFail-Isom L, Sines CC, Howerton SB, Stephens RK, Williams LD. Monovalent cations sequester within the A-tract minor groove of $[CGCGAATTCGCG)]_2$. J. Am. Chem. Soc 2000;122:1546–1547.
10. Howerton SB, Sines CC, Vanderveer D, Williams LD. Locating monovalent cations in the grooves of B-DNA. Biochemistry 2001;40:10023–10031. [PubMed: 11513580]
11. Marincola FC, Denisov VP, Halle B. Competitive Na^+ and Rb^+ binding in the minor groove of DNA. J. Am. Chem. Soc 2004;126:6739–6750. [PubMed: 15161302]
12. Dickerson RE, Drew HR. Structure of a B-DNA dodecamer. II. Influence of base sequence on helix structure. J. Mol. Biol 1981;149:761–786. [PubMed: 6273591]
13. Shui X, McFail-Isom L, Hu GG, Williams LD. The B-DNA dodecamer at high resolution reveals a spine of water on sodium. Biochemistry 1998;37:8341–8355. [PubMed: 9622486]
14. Shui X, Sines CC, McFail-Isom L, VanDerveer D, Williams LD. Structure of the potassium form of CGCGAATTCGCG: DNA deformation by electrostatic collapse around inorganic cations. Biochemistry 1998;37:16877–16887. [PubMed: 9836580]
15. Young MA, Jayaram B, Beveridge DL. Intrusion of counterions into the spine of hydration in the minor groove of B-DNA: fractional occupancy of electronegative pockets. J. Am. Chem. Soc 1997;119:59–69.
16. Snoussi K, Leroy JL. Alteration of A·T base-pair opening kinetics by the ammonium cation in DNA A-tracts. Biochemistry 2002;41:12467–12474. [PubMed: 12369837]
17. Ponomarev SY, Thayer KM, Beveridge DL. Ion motions in molecular dynamics simulations on DNA. Proc. Natl. Acad. Sci. USA 2004;101:14771–14775. [PubMed: 15465909]
18. Lavery R, Pullman B. The dependence of the surface electrostatic potential of B-DNA on environmental factors. J. Biomol. Struct. Dyn 1985;2:1021–1032. [PubMed: 3916934]
19. Das R, Mills TT, Kwok LW, Maskel GS, Millett IS, Doniach S, Finkelstein KD, Herschlag D, Pollack L. Counterion distribution around DNA probed by solution x-ray scattering. Phys. Rev. Lett 2003;90:188103. [PubMed: 12786045]
20. Várnai P, Zakrzewska K. DNA and its counterions: a molecular dynamics study. Nucleic Acids Res 2004;32:4269–4280. [PubMed: 15304564]
21. Stellwagen NC, Magnusdó, Gelfi C, Righetti PG. Preferential counterion binding to A-tract DNA oligomers. J. Mol. Biol 2001;305:1025–1033. [PubMed: 11162111]
22. Stellwagen E, Lu YJ, Stellwagen NC. Curved DNA molecules migrate anomalously slowly in free solution. Nucleic Acids Res 2005;33:4425–4432. [PubMed: 16085753]
23. Stellwagen NC, Magnusdóttir, Gelfi C, Righetti PG. Measuring the translational diffusion coefficients of small DNA molecules by capillary electrophoresis. Biopolymers 2001;58:390–397. [PubMed: 11180052]
24. Lu YJ, Stellwagen NC. Monovalent cation binding by curved DNA molecules containing variable numbers of A-tracts. Biophys. J 2008;94:1719–1725. [PubMed: 17993492]
25. Stellwagen E, Dong Q, Stellwagen NC. Quantitative analysis of monovalent counterion binding to random-sequence, double-stranded DNA using the Replacement Ion method. Biochemistry 2007;46:2050–2058. [PubMed: 17253778]

26. Stellwagen E, Stellwagen NC. The free solution mobility of DNA in Tris-acetate-EDTA buffers of different concentrations, with and without added NaCl. Electrophoresis 2002;23:1935–1941. [PubMed: 12116139]
27. Stellwagen E, Stellwagen NC. Probing the electrostatic shielding of DNA with capillary electrophoresis. Biophys. J 2003;84:1855–1866. [PubMed: 12609887]
28. Tan ZJ, Chen SJ. Ion-mediated nucleic acid helix-helix interactions. Biophys. J 2006;91:518–536. [PubMed: 16648172]
29. Holmes DL, Stellwagen NC. Estimation of polyacrylamide gel pore size from Ferguson plots of normal and anomalously migrating DNA fragments I. Gels containing 3% N,N'-methylenebisacrylamide. Electrophoresis 1991;12:253–263. [PubMed: 2070781]
30. Dong Q, Stellwagen E, Dagle JM, Stellwagen NC. Free solution mobility of small single-stranded oligonucleotides with variable charge densities. Electrophoresis 2003;24:3323–3329. [PubMed: 14595678]
31. Stellwagen NC, Gelfi C, Righetti PG. The free solution mobility of DNA. Biopolymers 1997;42:687–703. [PubMed: 9358733]
32. Williams BA, Vigh G. Fast, accurate mobility determination method for capillary electrophoresis. Anal. Chem 1996;68:1174–1180.
33. Wyman, J.; Gill, SJ. Mill Valley, CA: University Science Books; 1990. Binding and Linkage.
34. Marky LA, Breslauer KJ. Origins of netropsin binding affinity and specificity: correlations of thermodynamic and structural data. Proc. Natl. Acad. Sci. USA 1987;84:4359–4363. [PubMed: 3037518]
35. Ward B, Rehfuss R, Goodisman J, Dabrowiak JC. Determination of netropsin-DNA binding constants from footprinting data. Biochemistry 1988;27:1198–1205. [PubMed: 2835086]
36. Rentzeperis D, Marky LA. Interaction of minor groove ligands to an AAATT/AATTT site: correlation of thermodynamic characterization and solution structure. Biochemistry 1995;34:2937–2945. [PubMed: 7893707]
37. Lah J, Vesnaver G. Energetic diversity of DNA minor-groove recognition by small molecules displayed through some model ligand-DNA systems. J. Mol. Biol 2004;342:73–80. [PubMed: 15313608]
38. Freyer MW, Buscaglia R, Chasman D, Hyslop S, Wilson WD, Chaires JB, Lewis EA. Binding of netropsin to several DNA constructs: evidence for at least two different 1:1 complexes formed from an –AATT-containing ds-DNA construct and a single minor groove binding ligand. Biophys. Chem 2007;126:186–196. [PubMed: 16837123]
39. Degtyareva NN, Fresia MJ, Petty JT. DNA conformational effects on the interaction of netropsin with A-tract sequences. Biochemistry 2007;46:15136–15143. [PubMed: 18044972]
40. Nguyen B, Tanious FA, Wilson WD. Biosensor-surface plasmon resonance: Quantitative analysis of small molecule-nucleic acid interactions. Methods 2007;42:150–161. [PubMed: 17472897]
41. Diekmann S. Sequence specificity of curved DNA. FEBS 1986;3244:53–56.
42. Koo HS, Wu HM, Crothers DM. DNA bending at adenine·thymine tracts. Nature 1986;329:501–506. [PubMed: 3960133]
43. Katahira M, Sugeta H, Kyogoku Y, Fujii S, Fujisawa R, Tomita K. One-and two-dimensional NMR studies of DNA containing the oligo(dA)oligo(dT) tract. Nucleic Acids Res 1988;16:8619–8632. [PubMed: 3419927]
44. Katahira M, Sugeta H, Kuyogoku Y. A new model for the bending of DNAs containing oligo(dA) tracts based on NMR observations. Nucleic Acids Res 1990;18:613–618. [PubMed: 2308847]
45. Chuprina VP, Lipanov AA, Fedoroff OY, Kim SG, Kintanar A, Reid BR. Sequence effects on local DNA topology. Proc. Natl. Acad. Sci. USA 1991;88:9087–9091. [PubMed: 1924372]
46. Stefl R, Wu H, Ravindranathan S, Sklenář V, Feigon J. DNA A-tract bending in three dimensions: solving the dA4T4 vs. dT4A4 conundrum. Proc. Natl. Acad. Sci. USA 2004;101:1177–1182. [PubMed: 14739342]
47. Hud NV, Sklenář V, Feigon J. Localization of ammonium ions in the minor groove of DNA duplexes in solution and the origin of DNA A-tract bending. J. Mol. Biol 1999;286:651–660. [PubMed: 10024440]

48. Denisov VP, Halle B. Sequence-specific binding of counterions to B-DNA. Proc. Natl. Acad. Sci. USA 2000;97:629–633. [PubMed: 10639130]

49. Nelson HCM, Finch JT, Luisi BF, Klug A. The structure of an oligo(dA)·oligo(dT) tract and its biological implications. Nature 1987;330:221–226. [PubMed: 3670410]

50. DiGabriele AD, Steitz TA. A DNA dodecamer containing an adenine tract crystallizes in a unique lattice and exhibits a new bend. J. Mol. Biol 1993;231:1024–1039. [PubMed: 8515463]

51. Feig M, Pettitt BM. Sodium and chlorine ions as part of the DNA solvation shell. Biophys. J 1999;77:1769–1781. [PubMed: 10512802]

52. Hamelberg D, McFail-Isom L, Williams LD, Wilson WD. Flexible structure of DNA: ion dependence of minor-groove structure and dynamics. J. Am. Chem. Soc 2000;122:10513–10420.

53. Hamelberg D, Williams LD, Wilson WD. Influence of the dynamic positions of cations on the structure of the DNA minor groove: sequence-dependent effects. J. Am. Chem. Soc 2001;123:7745–7755. [PubMed: 11493048]

54. Manning GS. The molecular theory of polyelectrolyte solutions with applications to the electrostatic properties of polynucleotides. Q. Rev. Biophys 1978;11:179–246. [PubMed: 353876]

55. Goodsell DS, Kopka ML, Dickerson RD. Refinement of netropsin bound to DNA: bias and feedback in electron density map interpretation. Biochemistry 1995;34:4983–4993. [PubMed: 7711020]

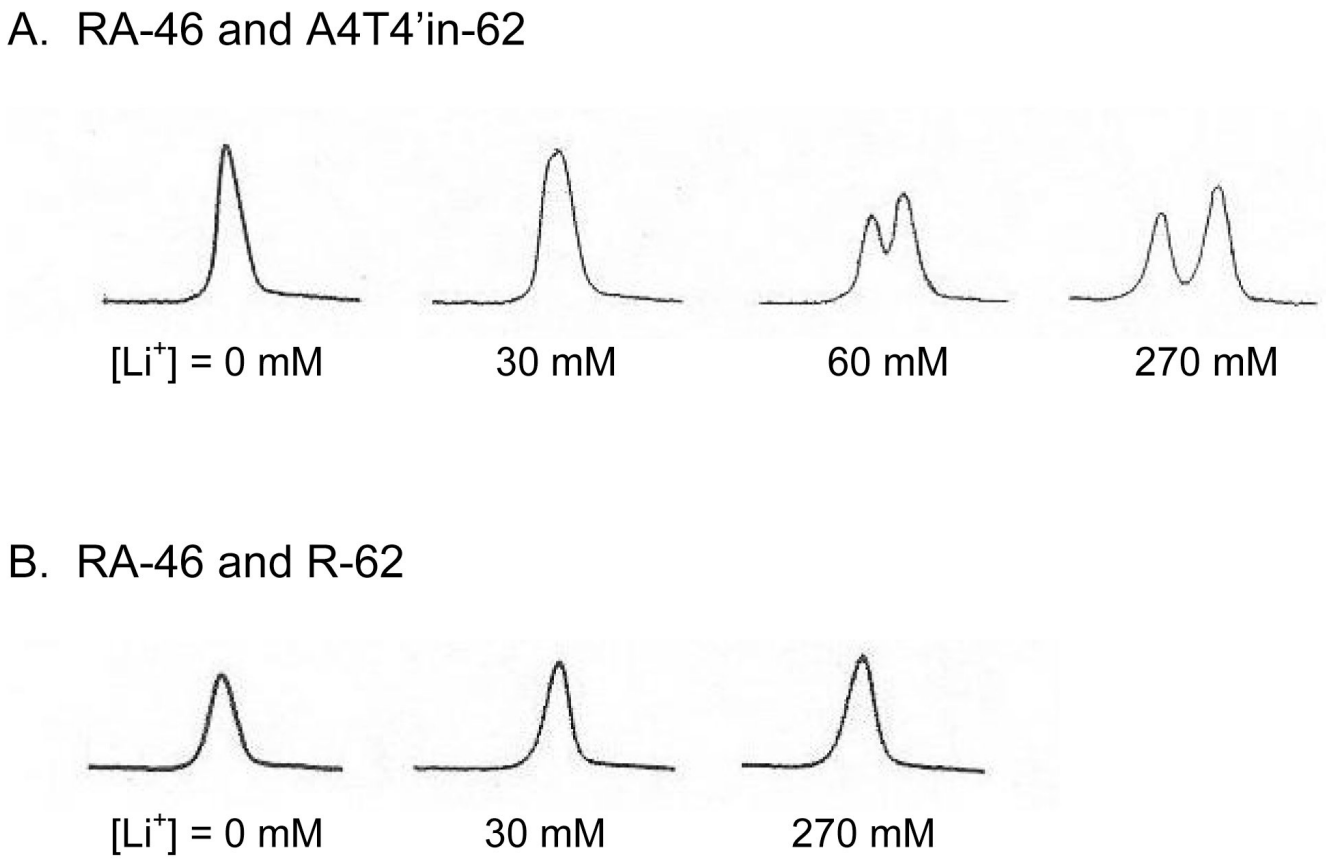

Figure 1.

Electropherograms observed for mixtures of RA-46 with: (A), A_4T_4'in-62; and (B), R-62. The leftmost electropherogram in each row corresponds to the mobility pattern observed when TPA^+ was the only cation in the BGE; the electropherograms to the right in each row were obtained with the indicated $[Li^+]$ in the BGE. The ordinate corresponds to optical density in arbitrary units; the abscissa corresponds to the time required for the peak(s) to migrate to the detector. The scales are the same for all electropherograms.

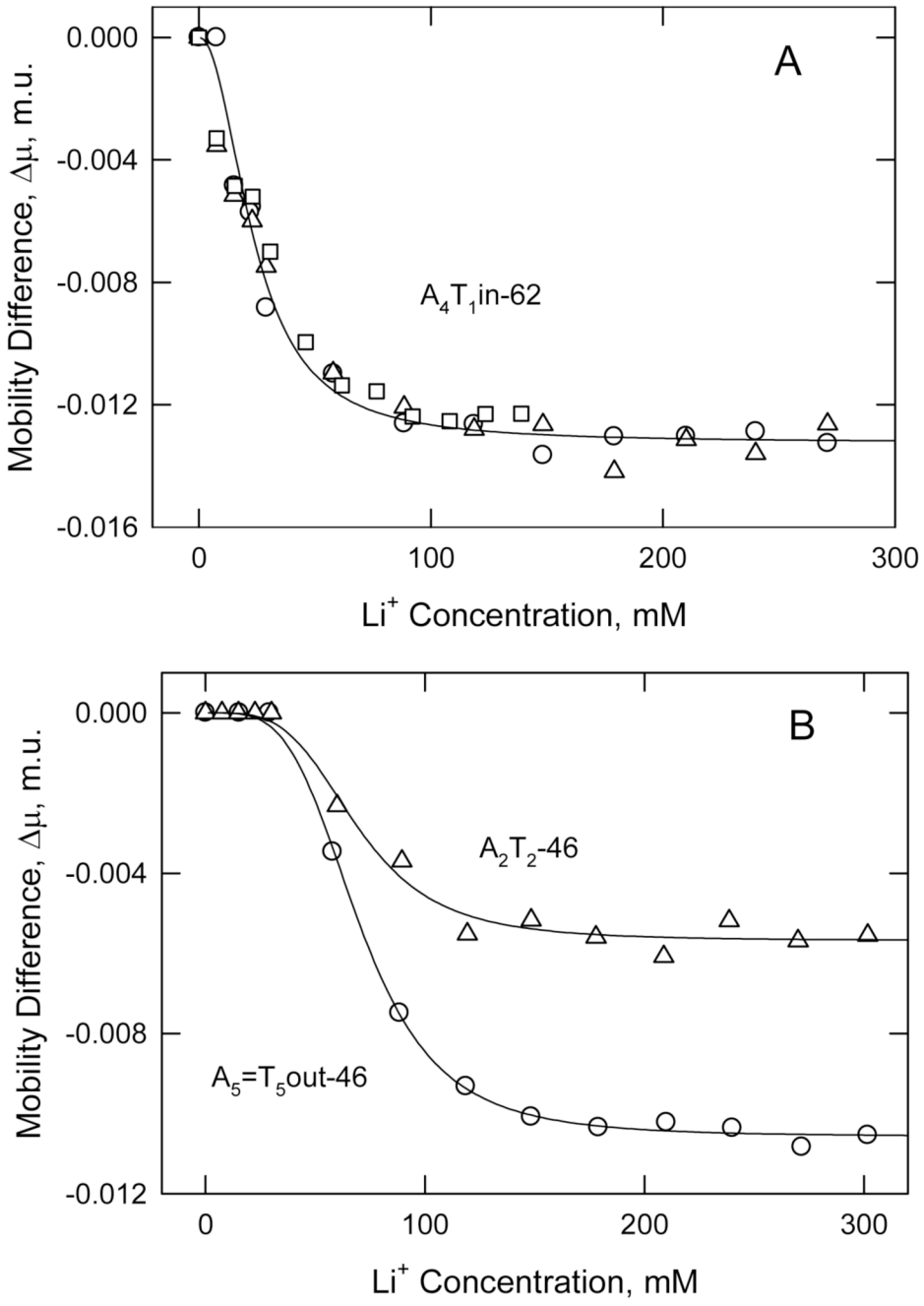

Figure 2.

Typical mobility profiles observed for A-tract-containing oligomers, using Li^+ as the binding ion. Mobility profiles are defined as the mobility difference (Δμ) between an A-tract-containing oligomer and RA-46, plotted as a function of binding ion concentration. (A), oligomer A4T2in-62, (o,Δ), two independent titrations in BGEs containing 300 mM cation; and (□), a BGE containing 150 mM cation. (B), Mobility profiles observed for oligomers A_2T_2-46 (Δ), and $A_5 = T_5$out-46 (o); the BGE contained 300 mM cation. The curved lines were drawn with eq 4; the corresponding ^{app}KD and $\Delta\mu_{max}$ values are given in Table 1 and Table 2. All mobility differences are given in mobility units; 1 m.u. = 1×10^{-4} cm^2 /Vs.

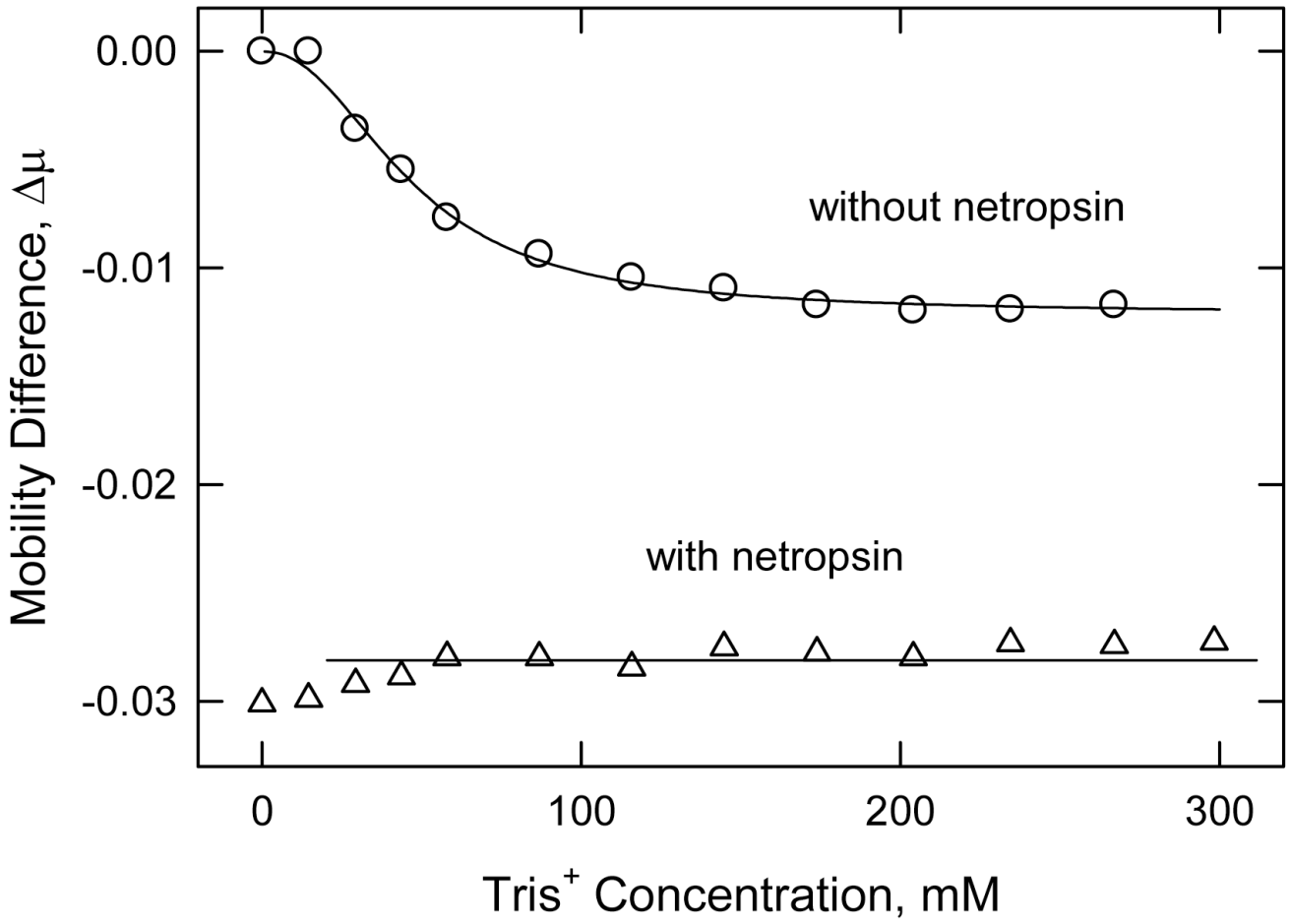

Figure 3.

Effect of netropsin on the mobility profiles obs;rved for oligomer A_4T_1in-62, using $Tris^+$ as the binding ion. (o), without netropsin; and (□), with netropsin added to the DNA. The curved line describing the Δμ values of oligomer A_4T_1in-62 (upper profile) were calculated from eq 4; the horizontal line (lower profile) corresponds to the average Δμ observed for the A_4T_1in-62/ netropsin complex at [$Tris^+$] concentrations > 15 mM.

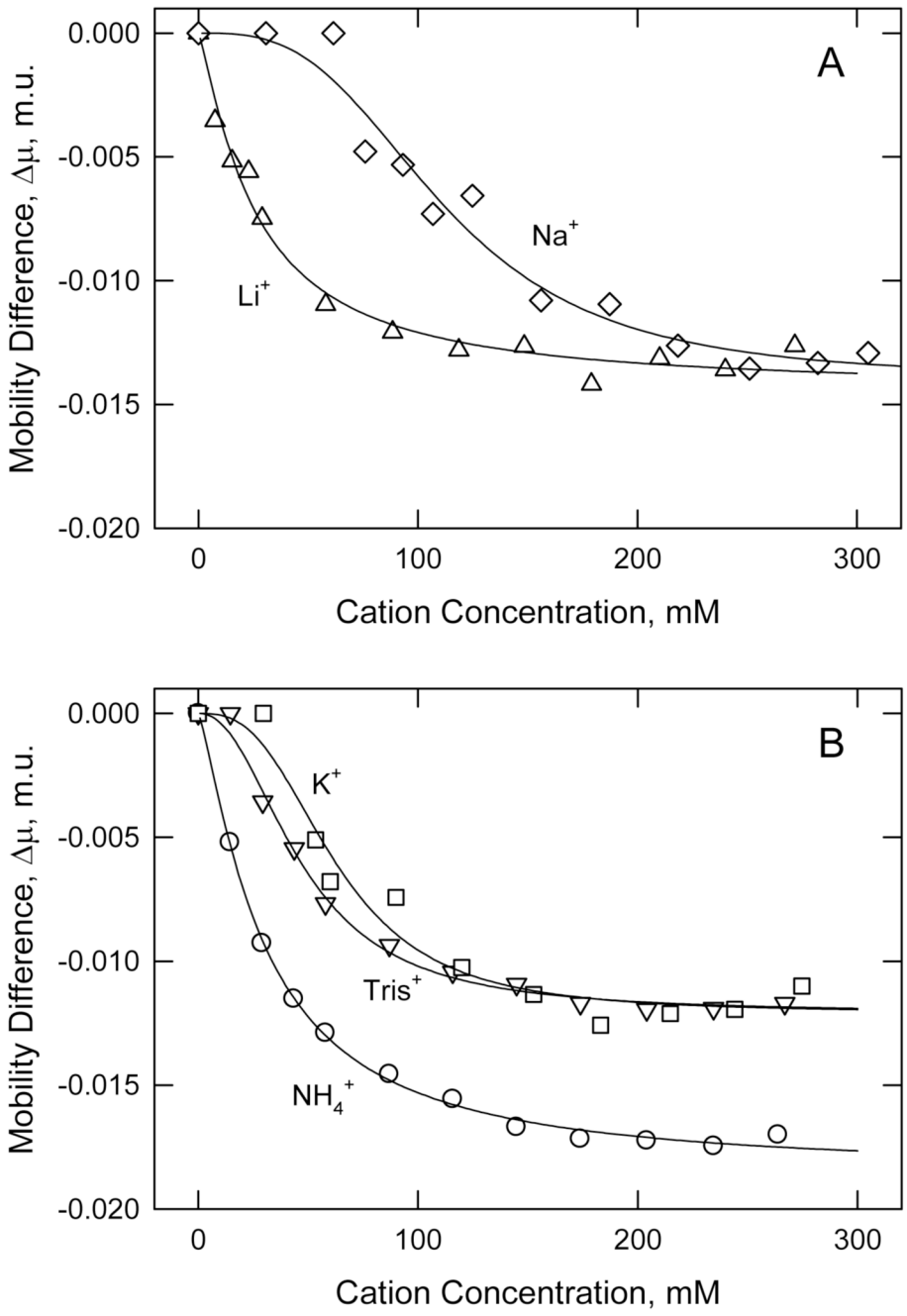

Figure 4.

Mobility profiles observed for the binding of different cations to oligomer A_4T_1in-62. The cations in (A) are: (Δ), Li^+; and (⋄), Na^+. The cations in (B) are: (o), NH_4^+; (∇), $Tris^+$; and (Δ), K^+. The curved lines were calculated from eq 4; the fitting parameters are given in Table 3.

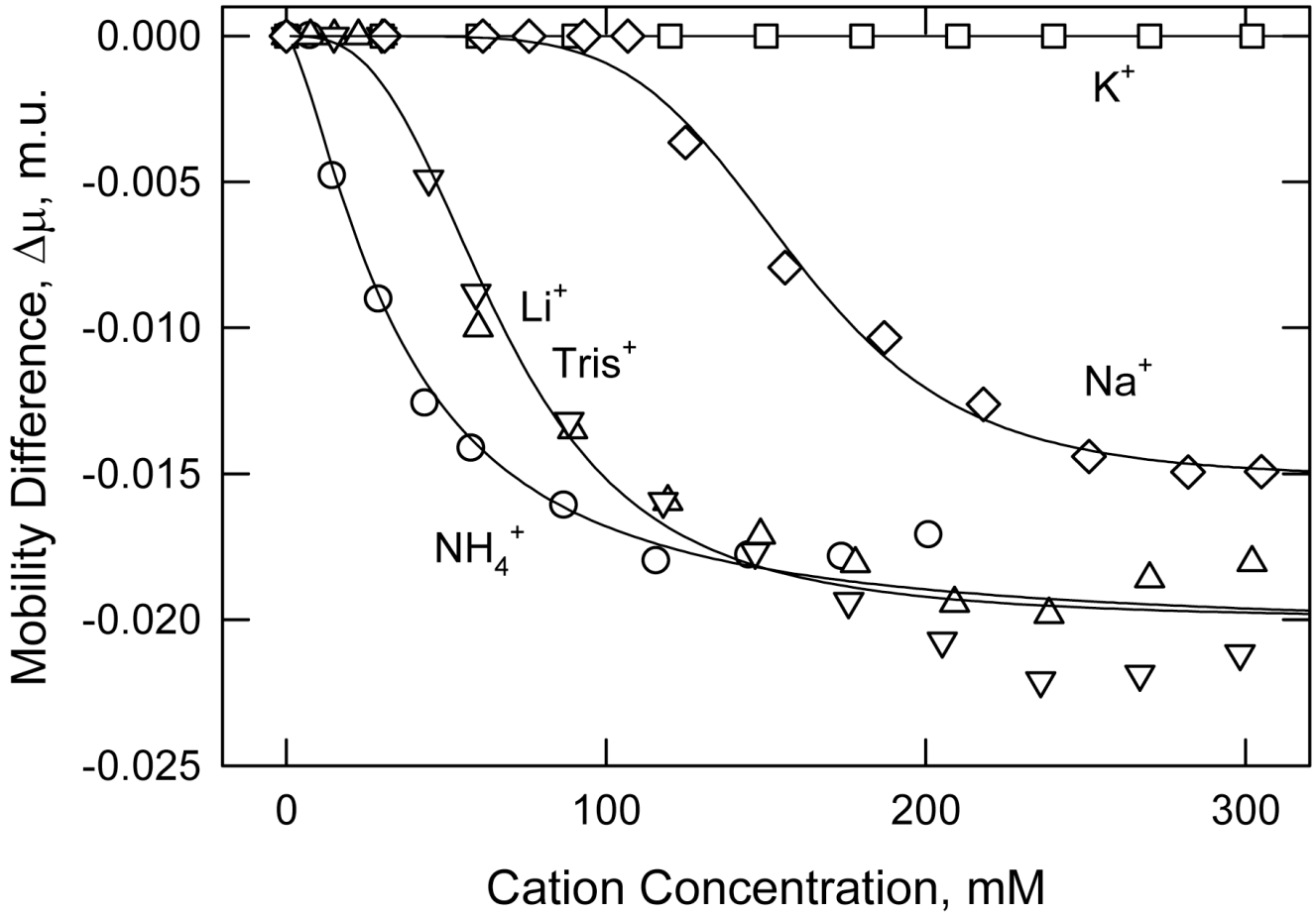

Figure 5.
Mobility profiles observed for the binding of various cations to oligomer A4T4'in-62. The binding cations are: (o), NH_4^+; (Δ), Li^+; (∇), $Tris^+$; (∇), Na^+; and (□), K^+. The curved lines were calculated from eq 4; the fitting parameters are given in Table 3.

Table 1

Sequences of oligomers containing 46% A+T, descriptive acronyms, and Li^+ ion binding constants.

Acronym	Sequence	$^{app}K_D$, mM	$-\Delta\mu_{max}$, m.u.
RA-46 (random)	CGCAGTGTACGACTAGACTACAGACG	n.b.[a]	---
A_4-46	CGCAAAAGCGTCGACACTAGTACTCG	51	0.0051
A_5-46	CGCAAAAAGCGTCGCACTAGTACTCG	65	0.0054
A_6-46	CGCAAAAAAGCGTCGCCTAGTACTCG	46	0.0082
A_7-46	CGCAAAAAAAGCGTCGCTCGTACTCG	55	0.0090
A_2T_2-46	CGCAATTCTATATGCTCCGCAGACCG	68	0.0060
A_3T_3-46	CGCAAATTTCTATGCTCCGCAGACCG	78	0.0100
A_4T_4-46	CGCAAAATTTTCTGCTCCGCAGACCG	78	0.0130
A_5T_5-46	CGCAAAAATTTTTACTCGCCGCGCCG	74	0.0130
A_3in-46	CGCAAAGCGTACGAAACTCTGTCTCG	100	0.0073
A_4in-46	CGCAAAAGCGTCGAAAACCTCTCTCG	41	0.0121
A_5in-46	CGCAAAAAGCCGCAAAAACCTCGTCG	71	0.0112
A_5out-46	CGCAAAAAGCCGCCTGAAAAACCTCG	71	0.0109
T_5in-46	CGCTTTTTGCCGCTTTTTCCAGCACG	100	0.0082
A_2T_2in-46	CGCAATTCGTCACAATTCTGCGACCG	128	0.0102
A_3T_3in-46	CGCAAATTTCGCCAAATTTCGCGCCG	97	0.0163
A_5=T_5in-46	CGCAAAAAGCTCGTTTTTCCGCACCG	67	0.0145
A_5=T_5out-46	CGCAAAAAGCTCGCCTTTTTGCACCG	69	0.0106
A_4T_1in-46	CGCAAAATCGGTCAAAATCGGCTGCG	131	0.0084

[a] n.b. = no binding

Table 2

Sequences of oligomers containing 62% A+T, descriptive acronyms and Li^+ ion binding constants.

Acronym	Sequence	$^{app}K_D$, mM	$-\Delta\mu_{max}$, m.u.
R-62 (random)	CGCTTACTAGATACTACTAGTACTAG	n.b.[a]	---
A_4T_1-62	CGCAAAATCTGATCATATGTACTTCG	50	0.0050
A_4T_3-62	CGCAAAATTTCTGATCATCATGATCG	64	0.0050
A_4T_4-62	CGCAAAATTTTCTGATCATCAGATCG	68	0.0070
A_4T_5-62	CGCAAAATTTTTCGATCATCAGATCG	57	0.0075
A_4in-62	CGCAAAAGTGTCTAAAATCTGTTCTG	54	0.0096
A_4T_1in-62	CGTAAAATCTGTGAAAATCTGTCTCG	24	0.0133
A_4T_2in-62	CGCAAAATTCGTCAAAATTCTGTCTG	73	0.0117
A_4T_3in-62	CGCAAAATTTGTCAAAATTTCGCTCG	58	0.0120
A_4T_4in-62	CGCAAAATTTTCGAAAATTTTCGCCG	64	0.0153
A_4T_4in-62	CGCCGCAAAATTTTCGAAAATTTTCG	58	0.0195
A_4T_4out-62	CGCAAAATTTTCGCGCAAAATTTTCG	54	0.0157
A_4T_4/T_4A_4in-62	CGCAAAATTTTCGTTTTAAAACGCCG	100	0.0092
A_3T_3in-62	CGCAAATTTCGACAAATTTCTAGTCG	85	0.0085
A_3T_3out-62	CGCAAATTTCGAGTCAAATTTCTACG	65	0.0090

[a] n.b. = no binding

Table 3

Comparison of binding constants observed for different cations.

	A_4T_1in-62			A_4T_4'in-62		
Cation	**$^{app}K_D$, mM**	**−Δμmax, m.u.**	***n***	**$^{app}K_D$, mM**	**$-\Delta\mu_{max}$, m.u**	***n***
NH_4^+	30	0.0186	1.3	35	0.0205	1.4
Li^+	26	0.0145	1.2	68	0.0200	3.0
$Tris^+$	47	0.0121	2.2	68	0.0200	3.0
Na^+	112	0.0140	3.1	159	0.0151	5.9
K^+	63	0.0121	2.8	>300	---	---